Stochastic classical trajectory approach to relaxation phenomena. II. Vibrational relaxation of impurity molecules in Debye solids

Abraham Nitzan[a)]

Department of Chemistry, Tel Aviv University, Tel Aviv, Israel and Bell Laboratories, Murray Hill, New Jersey 07974

Mary Shugard and John C. Tully

Bell Laboratories, Murray Hill, New Jersey 07974
(Received 12 May 1978)

The stochastic classical trajectory approach is extended through introduction of a systematic class of phonon mode densities. Convenient algorithms are presented for generating the required random forces and damping integrals corresponding to mode spectra which approach, as closely as desired, the Debye spectrum. Extension to realistic mode densities involving irregular and discontinuous features is discussed. Application to vibrational relaxation of impurities in solids demonstrates that rates can depend sensitively on the structure of the phonon density of states, particularly at low temperatures.

I. INTRODUCTION

In two recent papers,[1,2] we have applied the method of stochastic classical trajectories, first proposed by Adelman and Doll,[3] to the study of interactions of a foreign atom or molecule with a solid. In the first paper, the scattering and adsorption of atoms on solid surfaces was examined.[1] Related studies have been reported by others.[4-6] In the second[2] (paper I of this series), we applied the same approach to the study of vibrational relaxation of impurity molecules in the bulk of a solid matrix. The assumption taken in paper I is that the two major factors which determine the relaxation process are the interaction of the impurity molecule with its nearest neighbors and the gross features of the solid density of vibrational modes. Thus, the details of the solid structure are disregarded and the dynamics of a small system including the impurity molecule and its nearest neighbors is followed in the presence of random forces and damping kernels which account for the effects of the rest of the lattice. The random forces and damping kernels have to be constructed so that they represent realistically the effect of an infinite collection of lattice modes with the appropriate density of states.

The construction of random forces and damping kernels that satisfy the above requirement and are computationally feasible is not straightforward. In the former works, we have simulated the solid by random force and damping which are characterized by a spectral density of form

$$g(\omega)=\frac{2}{\pi}\frac{\omega^2\Lambda_c(\omega)}{[\omega^2-\Omega^2-\omega\Lambda_s(\omega)]^2+\omega^2\Lambda_c^2(\omega)}\ , \tag{I.1}$$

where

$$\Lambda_c(\omega)=\Lambda_0\frac{\beta\omega_0^2}{(\omega^2-\omega_0^2)^2+\beta^2\omega^2}\ , \tag{I.2}$$

and

$$\Lambda_s(\omega)=\Lambda_0\frac{\omega(\omega^2-\omega_0^2+\beta^2)}{(\omega^2-\omega_0^2)^2+\beta^2\omega^2}\ . \tag{I.3}$$

This form arises in the theory of the Brownian harmonic oscillator.[7] The parameters Ω, ω_0, β, and Λ_0 are chosen to achieve as close a fit as possible to a given spectrum (e.g., a Debye spectrum). The main deficiency of this density of states is the absence of a sharp cutoff at high frequency. Instead, Eqs. (I.1)–(I.3) exhibit a high frequency tail which falls off as ω^{-6}. This is likely to be unimportant for processes like atom–surface scattering and desorption for which the atom–solid interaction takes place in a relatively short time interval. The absence of a sharp cutoff in the spectral density at high frequency will introduce errors only in the long-time correlations, so Eqs. (I.1)–(I.3) should be acceptable in situations where long-time correlation effects play a minor role. On the other hand, the vibrational relaxation of impurity molecules imbedded in a solid is a relatively long-time process in which the interaction is always present. This implies that the detailed features of the density of states function may be important in determining the nature of the relaxation process. The most important feature, of course, is the sharp Debye cutoff. An impurity molecule with frequency ω above the entire range of frequencies of the solid (e.g., $\omega>\omega_D$ for a Debye solid) can decay only in the presence of anharmonic interactions. However, with the model density of states produced by Eqs. (I.1)–(I.3), the impurity frequency will always be imbedded in the ω^{-6} high frequency tail, resulting in some decay even in a totally harmonic system.

In the present paper, we describe a method by which the random force and damping functions can be constructed in a computationally feasible way for a solid with a spectral density which can approach a Debye spectrum as closely as we wish. This spectral density function is given by

$$g(\omega)=N\frac{\omega^2}{1+(\omega/\omega_D)^{2n}}\ , \tag{I.4}$$

a) Supported in part by the Commission for Basic Research of the Israeli Academy of Sciences, and by the Israel–USA Binational Science Foundation, Jerusalem, Israel.

 0021-9606/78/6906-2525$01.00

where ω_D is the Debye frequency and N is a normalization constant. As $n \to \infty$, $g(\omega)$ approaches a real Debye spectrum while the case $n=4$ produces a ω^{-6} tail, as with the model we used before [Eqs. (I.1)–(I.3)]. The functions given by Eqs. (I.1)–(I.3) and by Eq. (I.4) for several n's are shown in Fig. 1.

What we mean by a computationally feasible model is one for which a procedure can be found such that the non-Markoffian stochastic equations, obtained when the original set of equations of motion is projected onto the small space consisting of the impurity and its relevant nearest neighbors, can be solved in a Markoffian way. In the following sections, we describe how this can be done for a solid characterized by the spectral density $g(\omega)$ of Eq. (I.4). Following this, we use the procedure to investigate the dependence of the relaxation process on the form of the density of modes function given by the choice of n in Eq. (I.4). It is found that, at zero temperature, lifetimes and, in fact, the full relaxation behavior are quite sensitive to the choice of n. The behavior at nonzero temperature is much less sensitive to n and $n=4$ seems to be sufficient for most high temperature studies. We repeat some of the studies of paper I and show that the qualitative conclusions concerning the parameter dependence of the relaxation rates remain intact even though the absolute rates may vary.

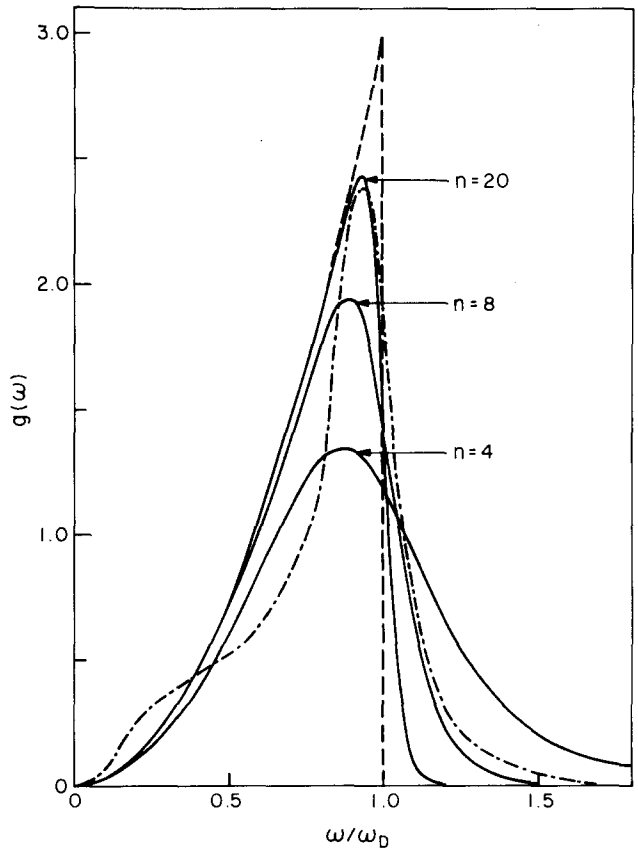

FIG. 1. Spectral densities obtained from Eq. (I.4) for various values of n. The dashed curve is the Debye spectrum. The dot–dash curve is from Eq. (I.1).

II. REDUCED REPRESENTATION OF LOCAL PROCESSES

In this section, we cast the equations of motion for the impurity molecule and the lattice atoms in a form which involves the coordinates of the impurity molecule and the lattice normal modes. We then replace the full dynamical description by a reduced form containing appropriate random forces and damping kernels. The procedure is essentially equivalent to the projection operator procedure used before.[1–3] However, it is done in a way that insures that the unperturbed motion of the nearest neighbor lattice atom is characterized by the spectrum (I.4). The method can be extended for more complicated density spectra characterized by cutoff behavior similar to that of Eq. (I.4), as discussed at the end of this section.

For simplicity, we start with a one-dimensional example in which one impurity coordinate x is coupled through a potential $U[x-(R_l^{eq}+y_l)]$ to the coordinate y_l, which measures the deviation of a lattice atom from its equilibrium position R_l^{eq} in the lth lattice site. The equations of motion of the free harmonic lattice can be written quite generally in the form

$$\ddot{y}_k = -\sum_{k'} A_{kk'} y_{k'} \ . \tag{II.1}$$

In the presence of the impurity atom, the equations of motion become

$$\ddot{x} = -\frac{1}{m}\frac{\partial U[x(R_l^{eq}+y_l)]}{\partial x} \ , \tag{II.2}$$

$$\ddot{y}_l = -\sum_{l'} A_{ll'} y_{l'} - \frac{1}{M_l}\frac{\partial}{\partial y_l} U[x-(R_l^{eq}+y_l)] \ , \tag{II.3}$$

$$\ddot{y}_k = -\sum_{l'} A_{kl'} y_{l'} \quad (k \neq l) \ , \tag{II.4}$$

where m is the impurity and M_l is the lattice atom masses. The coefficients A_{ij} appearing in Eqs. (II.3) and (II.4) are, in general, different from those corresponding to the free lattice [Eq. (II.1)]. Equations (II.3) and (II.4) can be rewritten in the form

$$\ddot{\mathbf{y}} = \mathbf{A}\,\mathbf{y} + \mathbf{b} \ , \tag{II.5}$$

with

$$b = -\begin{pmatrix} \frac{1}{M_1}\frac{\partial U}{\partial y_1} \\ \vdots \\ \frac{1}{M_l}\frac{\partial U}{\partial y_l} \\ \vdots \end{pmatrix} = -\begin{pmatrix} 0 \\ \vdots \\ 0 \\ \frac{1}{M_l}\frac{\partial U}{\partial y_l} \\ 0 \\ \vdots \\ 0 \end{pmatrix} \ . \tag{II.6}$$

Let S be the (Hermitian) matrix which diagonalizes $\mathbf{A}$:

$$\mathbf{S}\,\mathbf{A}\,\mathbf{S}^{-1} = \mathbf{D} \ \text{(diagonal)} \ . \tag{II.7}$$

Define

$$\mathbf{S}\,\mathbf{y} = \mathbf{z} \tag{II.8}$$

so that

$$\frac{\partial z_k}{\partial y_j} = S_{kj} \ . \tag{II.9}$$

Then, from Eq. (II.5), we obtain the equations of motion for the **z** coordinates

$$\ddot{z}_k = -D_k z_k - \frac{\partial z_k}{\partial y_l}\frac{1}{M}\frac{\partial U}{\partial y_l} \tag{II.10}$$

or

$$\ddot{z}_k = -D_k z_k + \frac{S_{kl}}{M}\frac{\partial U}{\partial x} \ . \tag{II.11}$$

Putting $D_k = \omega_k^2$, ω_k is seen to be the frequency of the normal mode k in the lattice characterized by a vacant site at the equilibrium position of the impurity atom. The formal solution of Eq. (II.11) is

$$z_k(t) = z_k(0)\cos(\omega_k t) + \frac{1}{\omega_k}\dot{z}_k(0)\sin(\omega_k t) + \frac{S_{kl}}{M}\int_0^t d\tau \left(\frac{\partial U}{\partial x}\right)_\tau \frac{\sin[\omega_k(t-\tau)]}{\omega_k} \ . \tag{II.12}$$

Multiplying by S_{kl}^* and summing over all k, we get

$$y_l(t) = \sum_k S_{kl}^*\left[z_k(0)\cos(\omega_k t) + \frac{1}{\omega_k}\dot{z}_k(0)\sin(\omega_k t)\right] + \frac{1}{M}\int_0^t dt \left(\frac{\partial U}{\partial x}\right)_\tau F(t-\tau) \ , \tag{II.13}$$

where

$$F(t) = \sum_k |S_{kl}|^2 \frac{\sin(\omega_k t)}{\omega_k} = \int d\omega g(\omega)\frac{\sin(\omega t)}{\omega} \ , \tag{II.14}$$

with $g(\omega)$ being a weighted density of modes function defined from this equation. Equations (II.2) and (II.13) constitute a set equivalent to the original set of equations of motion (II.2)–(II.4).

Consider now the function

$$R_l(t) = \sum_k S_{kl}^*\left[z_k(0)\cos(\omega_k t) + \frac{1}{\omega_k}\dot{z}_k(0)\sin(\omega_k t)\right] \ , \tag{II.15}$$

which contributes to the rhs of Eq. (II.13). Knowing the transformation matrix **S** and given $z_k(0)$ and $\dot{z}_k(0)$ for each k, $R_l(t)$ is a completely deterministic function. In fact, the initial values $z_k(0)$ and $\dot{z}_k(0)$ can be separated into two parts each: a systematic part which describes an actual given initial deviation from equilibrium and a random part which vanishes at zero temperature. In what follows, we assume that the systematic part of $R_l(0)$ vanishes. (See Appendix A for a discussion of the modification which follows otherwise.) In this case, $z_k(0)$ and $\dot{z}_k(0)$ are Gaussian random variables which satisfy.

$$\langle z_k \rangle = \langle \dot{z}_k \rangle = 0 \ , \tag{II.16}$$

$$\langle |z_k|^2 \rangle = k_B T/M\omega_k^2 \ , \tag{II.17}$$

$$\langle |\dot{z}_k|^2 \rangle = k_B T/M \ , \tag{II.18}$$

with all the mixed correlation functions being zero. Therefore, $R_l(t)$ is also a Gaussian random process with

$$\langle R_l(t) \rangle = 0 \tag{II.19}$$

and

$$\langle R_l(t) R_l(0) \rangle = \sum_k |S_{kl}|^2 \langle |z_k(0)|^2 \rangle \cos(\omega_k t) = \frac{k_B T}{M}\sum_k |S_{kl}|^2 \frac{\cos(\omega_k t)}{\omega_k^2} = \frac{k_B T}{M}\int d\omega \frac{g(\omega)}{\omega^2}\cos(\omega t) \ . \tag{II.20}$$

In a free lattice, $g(\omega)$ is just the density of modes function for that lattice. Even for this case it is not generally known. However, we expect that for our needs the most important feature of $g(\omega)$ is its truncated behavior. We therefore model this function by Eq. (I.4) which approaches a Debye spectrum for $n \to \infty$. We note in passing that this is a model spectrum for a three-dimensional lattice so that the $3D$ feature of the system is introduced at this point.

Another important assumption which is necessary for reducing the complexity of the computational problem is made at this point. Rather than performing the integration of the equations of motion for a given set of initial conditions $\{z_k(0)\}$, $\{\dot{z}_k(0)\}$ and then averaging over the ensemble of initial conditions, we regard the equation

$$y_l(t) = R_l(t) + \frac{1}{M}\int_0^t d\tau \left\{\frac{\partial U[x - (R_l^{eq} + y_l)]}{\partial x}\right\}_{\substack{x=x(\tau) \\ y=y_l(\tau)}} F(t-\tau) \tag{II.21}$$

as a stochastic integral equation for y_l, with $R_l(t)$ playing the role of a Gaussian random "force" characterized by Eq. (II.19) and (II.20). The numerical procedure should generate this random process during the integration step by step.

So far we have discussed a one-dimensional problem of a single impurity atom coupled to the lattice through a single lattice atom. To get closer to the real physical situation without adding yet to the mathematical complexity of the problem, we consider the same model used in paper I. It consists of a diatomic molecule substituting a single atom in a monoatomic lattice and makes use of the following simplifying assumptions: (a) The interaction between the impurity molecule and the lattice is an additive combination of atom pair interactions with nearest neighbor lattice atoms. (b) Only interactions with nearest neighbors seated along the impurity axis are considered and impurity rotations and librations are disregarded. (c) Each lattice atom which interacts with the impurity is coupled to its own lattice. We thus neglect correlations between the motion of the lattice atoms except those generated by their coupling through the impurity.

These assumptions, their implications, and the extent to which they can be relaxed were discussed in paper I. The model now consists of a diatomic impurity molecule coupled by atom pair interactions to two lattice atoms in a collinear geometry as shown in Fig. 2. The two lattice atoms are coupled each to its own model three dimensional lattice. The equations of motion become

$$\ddot{x}_a = -\frac{1}{m_a}\left[\sum_{l=1}^{2}\frac{\partial U_{al}}{\partial x_a} + \frac{\partial}{\partial x_a}V(|x_a - x_b|)\right] \ , \tag{II.22}$$

$$\ddot{x}_b = -\frac{1}{m_b}\left[\sum_{l=1}^{2}\frac{\partial U_{bl}}{\partial x_b} + \frac{\partial}{\partial x_b}V(|x_a - x_b|)\right] \ , \tag{II.23}$$

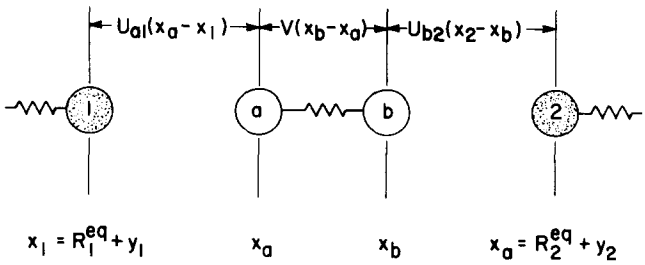

FIG. 2. Coordinates defining the four-atom model. Atoms 1 and 2 are host atoms, atoms a and b are impurity atoms.

$$y_l(t) = R_l(t) + \frac{1}{M}\int_0^t d\tau \left(\frac{\partial U_{al}}{\partial x_a} + \frac{\partial U_{bl}}{\partial x_b}\right)_\tau F(t-\tau) \ , \qquad \text{(II.24)}$$

with

$$U_{nl} = U[|x_n - (R_l^{eq} + y_l)|] \ , \quad n = a, b \ , \qquad \text{(II.25)}$$

and with R_l satisfying Eqs. (II.19) and (II.20) and F satisfying Eq. (II.14). V is the intramolecular potential which determines the internal motion of the diatomic impurity. Both U and V were assumed to depend on the absolute value of the distance between the corresponding atom pair. In the actual calculations of the present work, we used the same model potentials as in paper I, namely, harmonic or Morse functions for V:

$$V = \begin{cases} \frac{1}{2}K(x_b - x_a - r_{eq})^2 & \text{(harmonic)}, \quad \text{(II.25a)} \\ D\{1 - \exp[-\alpha(x_b - x_a - r_{eq})]\}^2 & \text{(Morse)} \ , \quad \text{(II.25b)} \end{cases}$$

where r_{eq} is taken to be the equilibrium bond length of the free impurity molecule, and an exponential repulsive or a Lenndard Jones functions for U:

$$U_{nl} = \begin{cases} A\exp(-\alpha|x_n - x_l|) & \text{(exponential)}, \quad \text{(II.26a)} \\ 4\epsilon\left[\left(\frac{\sigma}{x_n - x_l}\right)^{12} - \left(\frac{\sigma}{x_n - x_l}\right)^{6}\right] & \text{(Lennard-Jones)} \ , \quad \text{(II.26b)} \end{cases}$$

where $x_l = R_l^{eq} + y_l$. Equations (II.22)–(II.26) constitute the dynamical equations underlying the time evolution of our impurity lattice system. This is a set of stochastic integrodifferential equations which is in principle very difficult to solve numerically. The difficulties are associated with generating on the computer the random function $R_l(t)$ which satisfies Eqs. (II.19) and (II.20) and with calculating the integral appearing in Eq. (II.24), which is an integral over a memory kernel involving at any moment all the past history of the system. These difficulties limited us in paper I to considering the particular model [Eqs. (I.1)–I.3)] for the density of modes function for which a convenient algorithm could be found by which the computation could be carried out by solving an enlarged set of simple differential equations.[1] In the following section we describe a procedure for doing the same for the model defined by Eq. (I.4).

To end this section, we note again that a Debye spectrum is not a realistic model of the lattice mode density. General trends like the dependence on the impurity frequency and on the temperature are expected to be determined mainly by the truncated nature of the density of modes. Absolute rates as well as fine details of the general trends can depend, of course, on the detailed nature of the phonon spectrum, particularly on the presence of local or resonance modes. It should be kept in mind that some of these features are implicit in our present model: The local or resonance mode associated with the one-dimensional interaction of the impurity molecule with the approximately Debye solid is part of the dynamics described by Eqs. (II.22)–(II.24). We can build in more structure to the density of states function by considering a bigger cluster of lattice atoms as part of the dynamical system, attaching a Debye lattice to the end atoms of this dynamical cluster. As in paper I, this can be done in a way that will leave some free parameters that can be fitted to a desired density of modes function while still retaining the essential truncated behavior as given by Eq. (I.4).

III. COMPUTATION OF THE RANDOM NOISE AND THE LATTICE RESPONSE FUNCTIONS

In this section, we describe procedures for calculating the random function $R_l(t)$ and the lattice response function [the integral term in Eq. (II.24)] by reducing them to sets of Markoffian differential equations. We note that these two functions are interrelated as both essentially describe lattice vibrational properties. The formal connection is given by the relation (II.14) and (II.20) from which we obtain

$$F(t) = -\frac{M}{k_B T}\frac{d}{dt}\langle R_l(t) R_l(0)\rangle \ . \qquad \text{(III.1)}$$

It is therefore important to evaluate the lattice response and random terms in a consistent manner.

A. Lattice response function

Consider a function of the form

$$U(t) = \frac{1}{M}\int_0^t dt\, F(t-\tau) f(\tau) \ , \qquad \text{(III.2)}$$

where $F(t)$ is given by Eq. (II.14) and $f(\tau)$ is any function. In Appendix A, we show that for the model (I.A) we have

$$F(t) = \frac{1}{\omega_D \sigma}\begin{cases} \sum_{p=0}^{(1/2)n-1} e^{-b_p x}\left[2a_p b_p \sin(a_p x) + (b_p^2 - a_p^2)\cos(a_p x)\right] & (n \text{ even}) \ , \\ \sum_{p=0}^{1/2(n-3)} e^{-b_p x}\left[2a_p b_p \sin(a_p x) + (b_p^2 - a_p^2)\cos(a_p x)\right] + \frac{1}{2}e^{-x} & (n \text{ odd}) \ , \end{cases} \qquad \text{(III.3)}$$

where

$$x=\omega_D t \ , \tag{III.4}$$

$$a_p=\cos\left[\frac{(2p+1)\pi}{2n}\right] , \tag{III.5}$$

$$b_p=\sin\left[\frac{(2p+1)\pi}{2n}\right] , \tag{III.6}$$

and

$$\sigma=\left(2\sin\frac{3\pi}{2n}\right)^{-1} . \tag{III.7}$$

Now, define

$$S_p^s(t)=\int_0^t d\tau \exp[-b_p\omega_D(t-\tau)]\sin[a_p\omega_D(t-\tau)]f(\tau), \tag{III.8}$$

$$S_p^c(t)=\int_0^t d\tau \exp[-b_p\omega_D(t-\tau)]\cos[a_p\omega_D(t-\tau)]f(\tau), \tag{III.9}$$

$$S_e(t)=\int_0^t d\tau \exp[-\omega_D(t-\tau)]f(\tau) . \tag{III.10}$$

These function satisfy the differential equations

$$dS_p^s/dt = -b_p\omega_D S_p^s + a_p\omega_D S_p^c , \tag{III.11}$$

$$dS_p^c/dt = -b_p\omega_D S_p^c - a_p\omega_D S_p^s + f(t) , \tag{III.12}$$

$$dS_e/dt = -\omega_D S_e + f(t) , \tag{III.13}$$

with the initial conditions

$$S_p^s(t=0)=S_p^c(t=0)=0 \ \text{(all } p) ,$$

$$S_e(t=0)=0 . \tag{III.14}$$

In terms of these functions, the lattice response function $U(t)$ takes the form

$$U(t)=\frac{1}{M\omega_D\sigma}\begin{cases}\displaystyle\sum_{p=0}^{(1/2)n-1}[2a_p b_p S_p^s(t)+(b_p^2-a_p^2)S_p^c(t)] & (n \text{ even}) ,\\ \displaystyle\sum_{p=0}^{1/2(n-3)}[2a_p b_p S_p^s(t)+(b_p^2-a_p^2)S_p^c(t)]-\tfrac{1}{2}S_e(t) & (n \text{ odd}) .\end{cases} \tag{III.15}$$

Equations (III.11)–(III.15) with the definitions (III.5)–(III.7) reduce the calculation of $U(t)$ to an integration of a Markoffian system of differential equations which can be accomplished step by step together with the integration of the equations of motion.

B. Lattice random displacements

Next, we consider the random function $R(t)$ which we assumed to be a Gaussian random function satisfying [cf. Eqs. (II.20) and (II.21)]

$$\langle R(t)\rangle = 0 \tag{III.16}$$

and

$$\langle R(t)R(0)\rangle = \frac{k_B T}{M}\int_0^\infty d\omega\, g(\omega)\frac{\cos\omega t}{\omega^2} , \tag{III.17}$$

where $g(\omega)$ is again defined by Eq. (I.4), and its normalization constant is given by Eq. (A10). Our goal is to be able to generate R on the computer in a Markoffian way. This can be achieved in principle by having R as a member of a higher dimensional Markoff process.[7]

In Appendix B, we show that $R(t)$ can be obtained as the solution of the differential equation

$$\prod_{k=0}^{(n/2)-1}\left[\frac{d^2}{d(\omega_D t)^2}+2b_k\frac{d}{d(\omega_D t)}+1\right]R(t)=\rho(t) \quad (n \text{ even}) , \tag{III.18a}$$

$$\left[\frac{d}{d(\omega_D t)}+1\right]\prod_{k=0}^{(n-3)/2}\left[\frac{d^2}{d(\omega_D t)^2}+2b_k\frac{d}{d(\omega_D t)}+1\right]R(t)=\rho(t) \quad (n \text{ odd}), \tag{III.18b}$$

where $\rho(t)$ is a Gaussian Markoffian random process satisfying

$$\langle\rho(t)\rangle = 0 \tag{III.19a}$$

and

$$\langle\rho(t_1)\rho(t_2)\rangle = C\delta(t_1-t_2) , \tag{III.19b}$$

with C given by

$$C=\frac{k_B T}{M}\frac{2^{2(n-1)}2\sin\frac{3\pi}{2n}\prod_{l=1}^{n-1}\sin^2\frac{\pi l}{2n}}{\omega_D^3} . \tag{III.20}$$

The parameters b_k entering into Eqs. (III.18) are the same as those defined by Eq. (III.6). Equations (III.18) can also be written in the form

$$\left\{B_n^{[(n/2)-1]}\left[\frac{d}{d(\omega_D t)}\right]^n+B_{n-1}^{[(n/2)-1]}\left[\frac{d}{d(\omega_D t)}\right]^{n-1}+\cdots+B_1^{[(n/2)-1]}\frac{d}{d(\omega_D t)}+B_0^{(n/2)-1}\right\}R(t)=\rho(t) \tag{III.21a}$$

for n even and

$$\left\{D_n^{[(n-3)/2]}\left[\frac{d}{d(\omega_D t)}\right]^n+D_{n-1}^{[(n-3)/2]}\left[\frac{d}{d(\omega_D t)}\right]^{n-1}+\cdots+D_1^{[(n-3)/2]}\frac{d}{d(\omega_D t)}+D_0^{(n-3)/2}\right\}R(t)=\rho(t) \tag{III.21b}$$

for n odd. In these equations, the coefficients B satisfy the following recursion relations:

$$B_m^{(k)}=B_{m-2}^{(k-1)}+2b_k B_{m-1}^{(k-1)}+B_m^{(k-1)}, \quad m=2,3,4,\ldots,2k , \tag{III.22a}$$

$$B_{2k+1}^{(k)}=B_{2k-1}^{(k-1)}+2b_k B_{2k}^{(k-1)} , \tag{III.22b}$$

$$B_1^{(k)}=2b_k B_0^{(k-1)}+B_1^{(k-1)} \tag{III.22c}$$

$$B_{2k+2}^{(k)}=B_{2k}^{(k-1)}=1 , \tag{III.22d}$$

$$B_0^{(k)}=B_0^{(k-1)}=1 , \tag{III.22e}$$

while the D coefficients are given in terms of the B coefficients in the form

$$D_{n+1}^{[(n/2)-1]} = B_n^{[(n/2)-1]} = 1 \ . \qquad \text{(III. 23a)}$$

$$D_0^{[(n/2)-1]} = B_0^{[(n/2)-1]} = 1 \ , \qquad \text{(III. 23b)}$$

and

$$D_m^{[(n/2)-1]} = B_m^{[(n/2)-1]} + B_{m-1}^{[(n/2)-1]} \ , \quad m = 1, 2, \ldots, n \ . \qquad \text{(III. 23c)}$$

In Eqs. (III. 23), n is even.

In Eqs. (III. 21), R, the input into Eq. (III. 24), is obtained as a member of a n variable random process including also its first $n-1$ derivatives. To check the validity of the procedure, we have computed the Fourier transform of the correlation function $\langle R(t)R(0)\rangle$ after obtaining R from the numerical solution of Eq. (III. 18). From Eq. (III. 17), this should yield the density of modes function $g(\omega)$. The results from this computation are shown in Fig. 3.

The application of the method described here to the calculation of impurity relaxation in solid matrices is described in the following section.

IV. RESULTS AND DISCUSSION

The results of the computations based on Eqs. (II. 22)–(II. 24) are summarized in Figs. 4–7 and in Table I. To get these numbers, we ran trajectories of 10^4–10^5 points with a time increment of the order of $0.06\omega^{-1}$ (ω being the impurity frequency). Six to ten trajectories were used to average over the finite temperature behavior and the initial phase of the impurity oscillation. The longest run took about 15 sec of Honeywell 6000 computer time. In addition to averaging over trajectories, the instantaneous energy of the impurity was averaged over a time interval of the order of 5–10 impurity periods. This has the effect of eliminating the high frequency (and some low frequency) fluctuations from the energy relaxation curves. Since we did not exercise much averaging and used a rather small number of trajectories, the results obtained are accurate only to between 15% for the fastest relaxing zero temperature case and 40% for the

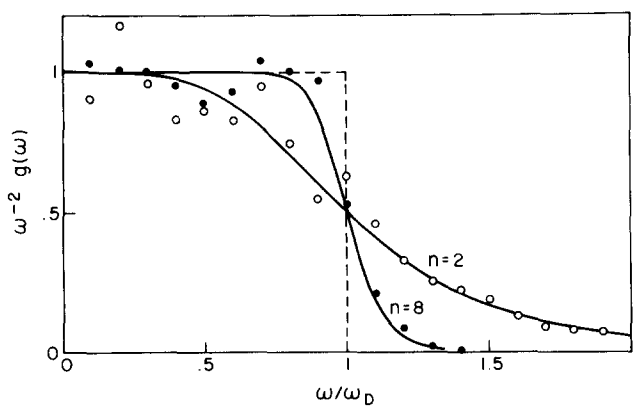

FIG. 3. Fourier transform of the position autocorrelation function $\langle R(t)R(0)\rangle$. Solid lines: $\omega^{-2}g(\omega)$ from Eq. (I. 4), for $n=2$ and $n=8$. Open and closed circles: results of numerical procedure of Sec. III for $n=2$ and 8, respectively. Scatter of points results from finite number of time steps sampled.

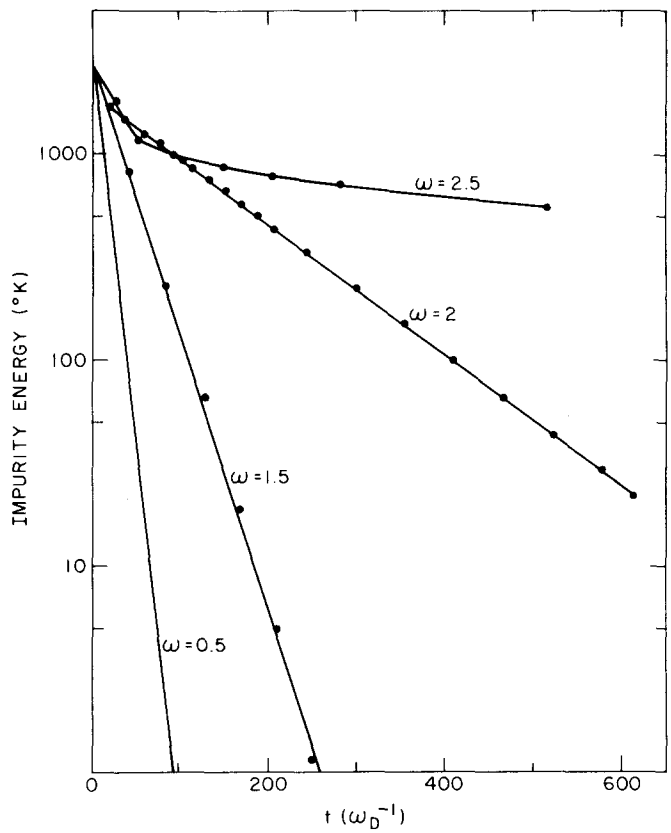

FIG. 4. Impurity energy as a function of time for $T=0$ °K, $n=4$, and several values of ω (in units of ω_D).

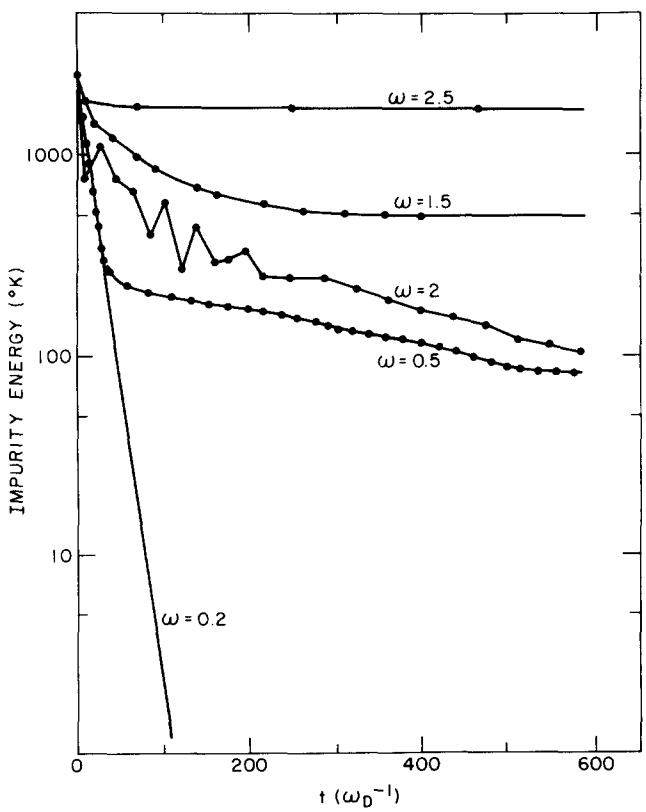

FIG. 5. Same as Fig. 4, but $n=18$.

TABLE I. Dependence of energy relaxation rates on n.[a]

n	Impurity frequency	Temp. (°K)	Rate (10^{10} sec^{-1})
4	$2\omega_D$	0	9.0
8	$2\omega_D$	0	b
12	$2\omega_D$	0	8.8
16	$2\omega_D$	0	4.3
20	$2\omega_D$	0	2.5
4	$2\omega_D$	20	36
10	$2\omega_D$	20	25
18	$2\omega_D$	20	18
4	$2\omega_D$	100	76
18	$2\omega_D$	100	30
4	$3\omega_D$	0	0.90
8	$3\omega_D$	0	6
12	$3\omega_D$	0	0.13
16	$3\omega_D$	0	0.15
20	$3\omega_D$	0	0.12
4	$3\omega_D$	10	7.0
12	$3\omega_D$	10	5.0

[a]Parameters used are $r_{eq}=2$ Å, and exponential coupling [Eq. (II. 26a)] with $A=8.0\times10^5$ eV and $\alpha=5.44$ Å^{-1}.
[b]Nonlinear behavior (see text).

slowest rates calculated. Faster finite temperature rates are good to within 20%–30%.

As a test case for computation, we took as in paper I a system with parameters similar to Cl_2 in the ground state ($r_{eq}=2.0$ Å) or in the excited B state ($r_{eq}=2.2$ Å) coupled to nearest neighbor argon lattice atoms by a Lennard-Jones potential with parameters appropriate to Ar–Ar interaction [$\epsilon=117.7$ °K and $\sigma=3.314$ Å in Eq. (II. 26a)], or an exponentially repulsive potential [Eq. (II. 26b)] with parameters chosen to fit the repulsive part of the Ar–Ar Lennard-Jones potential in the appropriate energy range ($A=8\times10^5$ eV, $\alpha=5.44$ Å^{-1}).

We found that replacing the Lennard-Jones potential by its repulsive part made only little change on the resulting rates and the rates reported here are based mostly on the repulsive interaction which is less time consuming in the computation.

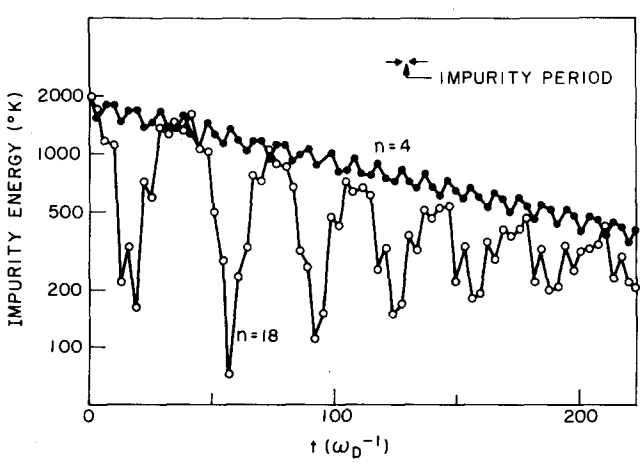

FIG. 6. Short-time behavior of impurity energy decay for $\omega=2\omega_D$ and $n=4$ or 18 at $T=0$ °K.

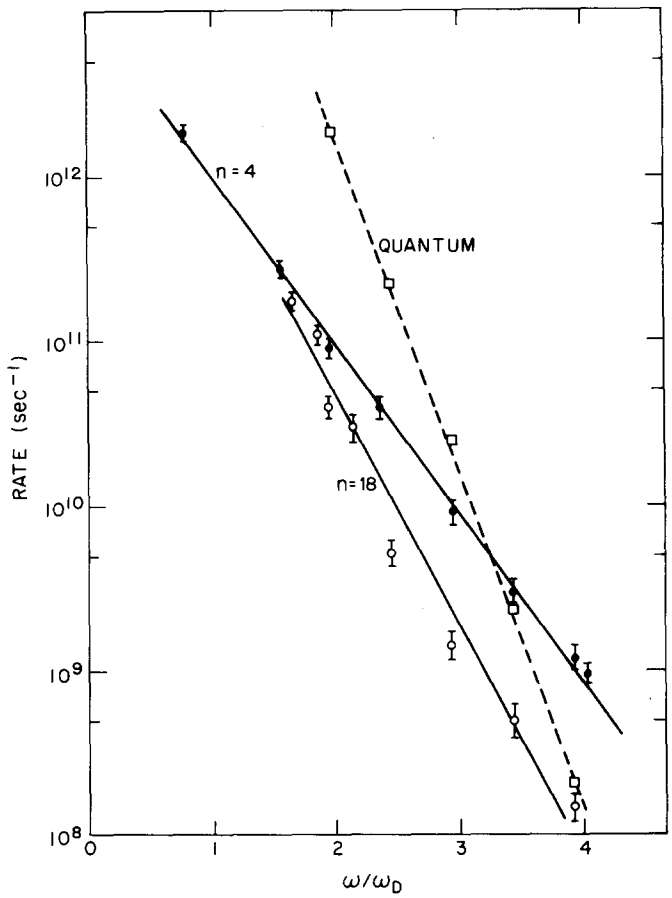

FIG. 7. Dependence of relaxation rate on impurity frequency ω for $n=4$ and $n=18$ at $T=0$ °K. The dashed line is from quantum mechanical perturbation theory of Ref. 9 (valid only for $\omega/\omega_D\gg1$) for a Debye lattice.

Table I gives the energy relaxation rates k defined from

$$dE/dt=-kE. \qquad \text{(IV. 1)}$$

where E is the total internal energy of the impurity molecule,[8] obtained for different choices of n in Eq. (I. 4) for a system characterized by Cl_2(ground state)–Ar parameters except that the impurity molecule is taken harmonic with $\omega=2$ or 3 (in units of $\omega_D=65$ cm^{-1}). This frequency corresponds to the energy spacing between higher vibrational levels of the Cl_2 molecule. We see that beyond some strange behavior (to be remarked upon later), the rates seem to be converging for high n. The convergence is better for higher ω as may be expected. It is also seen that, for nonzero temperatures, the rates obtained are much less sensitive to the choice of n.

Some decay curves obtained for different choices of ω are shown in Fig. 4 for $n=4$ and in Fig. 5 for $n=18$. It should be noted that the presence of a sharper cutoff in the phonon mode density in the $n=18$ case leads to a more fluctuating behavior of the relaxation curve. This was smoothed out to some extent by our averaging procedure, but is still present as shown in Fig. 6, where the short time behavior of the $\omega=2$, $n=4, 18$ cases is displayed.

The dependence of the relaxation rate on the harmonic frequency is displayed for the cases $n=4, 18$ in Fig. 7. It is seen that the qualitative behavior characterized by an exponential energy gap law is similar in both cases. However, the slope in the $n=18$ case is larger, as expected, so that the absolute rates are comparable for $\omega<2\omega_D$ while for $\omega\sim4\omega_D$ [order of the spacing between the lower vibrational levels of the Cl_2 in the excited $B\,^3\pi(O_u^+)$ state] they differ by an order of magnitude.

Figure 7 also shows the results of a quantum mechanical perturbation theory for a Debye lattice.[9] The quantum theory is expected to be accurate for large ω, and in fact is seen to predict rates similar to the $n=18$ calculations at the highest values of ω shown in Fig. 7.

The following conclusions can be drawn from these results: (1) The absolute rates and the relaxation pattern itself are very sensitive to the form of the density of states at zero temperature and are much less sensitive to it (i.e., to details which go beyond the presence of a cutoff at $\omega=\omega_D$) at finite temperatures. We should remember, however, that classical mechanics itself is probably not valid at temperatures approaching zero.[2]

The sensitivity to the structure of the density of states function appears to be an outcome of two factors. The unphysical tail in the density of states that we are using contributes a little to the rate and is responsible for the slow convergence of the large n behavior as seen in Table I. In addition, the close to singular structure of the function $g(\omega)$, especially for large n, may give rise to strange relaxation patterns usually characterized by a relatively rapid relaxation followed by very slow ones. For the case $n=18$, we found this behavior to characterize all impurity frequencies between $0.5\omega_D$ and $1.5\omega_D$ It is seen also in the cases marked "nonlinear behavior" in Table I. This behavior, which indicates trapping of localized trajectories and forming of quasilocal modes, is very sensitive to the functional form of $g(\omega)$ and we could not find a general pattern which will explain it. It should be mentioned that even though we do not find this behavior for larger impurity frequencies, the trajectories used in these cases are short relative to the relaxation time and we can not exclude the possibility that such nonlinear behavior also happens there. We do not expect this to be the case, however, because this behavior seems to be connected with a small distance between the impurity frequency and the lattice cutoff frequency. Nonlinear relaxation patterns associated with a small distance from a cutoff in a continuous spectrum are known also in other contexts.[10]

(2) General trends like the energy gap law, temperature dependence, and dependence on coupling parameters are qualitatively independent of the form of $g(\omega)$ and follow the pattern described in paper I. In particular, the relaxation rate of a harmonic impurity decreases exponentially with increasing ω. Rates for impurities of larger ω can be estimated roughly from plots like Fig. 7 by extrapolation of the "cheaper to calculate" rates of lower frequency fictitious impurities having the same coupling parameters.

V. CONCLUSION

In this work, we have extended the stochastic classical trajectory approach to vibrational relaxation in solids to include more realistic solid mode density models. The approach enabled us to study the effect of the model used. We have seen that the zero temperature absolute rates are very sensitive to the form of the density of modes of the solid. General trends like the dependence on potential parameters and on the nature of the impurity show only small sensitivity. Also, for nonzero temperatures, the dependence on the detailed form of the mode density is much weaker.

The method is still extendable in several directions. A three dimensional model which includes librational and rotational degrees of freedom is of interest. Also, more complicated density of modes functions with more structure can be constructed and fitted to actual densities of states. Finally, polyatomic impurity molecules can be considered and (matrix assisted) internal energy transfer can be studied. It should be noted that slow rates which are too expensive to calculate on the computer may possibly be estimated by extrapolation using, for example, the energy gap law (Fig. 7).

The main problems associated with the application of the present method lies in the need to know the structure of the impurity cavity and the form of the impurity lattice interaction potential. Another shortcoming is associated with our insufficient understanding of the problems related to the use of classical mechanics for this quantum mechanical problem. With an advance made in this last point, we expect the method to become a valuable tool in qualitative and even semiquantitative analysis of vibrational relaxation processes of impurity molecules in solids.

Finally, the method of stochastic classical trajectories has potential uses for other problems and fields. Being essentially a method for obtaining computer generated heat baths of various properties, it can be applied in a host of problems in statistical dynamics and offers a substantial saving in computation expenses relative to standard molecular dynamics calculations.

ACKNOWLEDGMENTS

We wish to thank Dr. V. Bondybey and Dr. E. Helfand for valuable discussions.

APPENDIX A. SYSTEMATIC INITIAL CONDITIONS

Consider Eq. (II. 13) in the form

$$y_I(t)=R_I^s(t)+R_I(t)+\int_0^t d\tau f(\tau)F(t-\tau)\,, \tag{A1}$$

where R now stands for the random part and R^s for the systematic part of the free modes motion and where $f=(1/M)(\partial U/\partial x)$. At $T=0$, $R_I=0$ and the systematic part is the only contribution to the unperturbed evolution of the initial conditions. This time evolution is given by

$$R_I^s(t)=\sum_k S_{kI}^*\left[z_k^s(0)\cos(\omega_k t)+\frac{1}{\omega_k}\dot{z}_k^s(0)\sin(\omega_k t)\right], \tag{A2}$$

where $z_k^s(0)$ and $\dot{z}_k^s(0)$ are the given initial amplitudes of

the different modes. An initial condition of practical importance for our purpose is obtained by imagining a constant force f operating on the lattice atom l before time zero. In the presence of such constant force and at $T=0$, $y_l(t)$ is given by

$$y_l(t)=\sum_k S_{kl}^*\left[z_k^s(0)\cos(\omega_k t) + \frac{1}{\omega_k}\dot{z}_k^s(0)\sin(\omega_k t)\right]+f\int_0^t d\tau F(\tau)\,. \tag{A3}$$

Inserting $F(t)$ from the first equality of Eq. (II. 14), we obtain

$$y_l(t)=\sum_k\left[S_{kl}^* z_k^s(0)-f|S_{kl}|^2\frac{1}{\omega_k^2}\right]\cos(\omega_k t) + \sum_k\frac{1}{\omega_k}\dot{z}_k(0)\sin(\omega_k t)+f\sum_k|S_{kl}|^2\frac{1}{\omega_k^2}\,. \tag{A4}$$

The magnitude of f is related to the normal mode amplitudes by the requirement that $y_l(t)$ is time independent in the presence of the stationary force f. Therefore,

$$y_l(0)=f\sum_k|S_{kl}|^2\frac{1}{\omega_k^2}\,, \tag{A5}$$

$$\dot{z}_k^s(0)=0 \quad (\text{all } k), \tag{A6}$$

$$z_k^s(0)=fS_{kl}\frac{1}{\omega_k^2}\,. \tag{A7}$$

Equation (A5) determines the magnitude of the fictitious force f in terms of the given $y_l(0)$

$$f=\left[\int d\omega\,\frac{g(\omega)}{\omega^2}\right]^{-1} y_l(0)\,. \tag{A8}$$

Inserting this into Eq. (A7), multiplying the latter by $S_{kl}^*\cos\omega_k t$, and summing over all k leads to

$$R_l^s(t)=\sum_k S_{kl}^* z_k^s(0)\cos(\omega_k t)=\beta(t)y_l(0)\,, \tag{A9}$$

with

$$\beta(t)=\left[\int d\omega\,\frac{g(\omega)}{\omega^2}\right]^{-1}\int d\omega\,\frac{g(\omega)}{\omega^2}\cos(\omega t)\,, \tag{A10}$$

or if $g(\omega)$ is given by an exact Debye spectral function

$$\beta(t)=\sin(\omega_D t)/\omega_D t\,. \tag{A11}$$

Thus, in the presence of a systematic initial deviation of y_l from zero, Eqs. (II. 13) and (II. 21) should be replaced by

$$y_l(t)=\beta(t)y_l(0)+R_l(t)+\frac{1}{M}\int_0^t d\tau\left(\frac{\partial U}{\partial x}\right)_\tau F(t-\tau)\,, \tag{A12}$$

and similarly a term $\beta(t)y_l(0)$ should be added into the rhs of Eq. (II. 24).

APPENDIX B. EVALUATION OF THE FUNCTION $F(t)$

Here, we outline the derivation of Eq. (III. 3) for $F(t)$, starting from

$$F(t)=\int_0^\infty d\omega\,\frac{g(\omega)}{\omega}\sin(\omega t)\,, \tag{B1}$$

with

$$g(\omega)=N\frac{(\omega/\omega_D)^2}{1+(\omega/\omega_D)^{2n}}\,. \tag{B2}$$

Defining

$$a(t)=\int_0^\infty d\omega\,\frac{g(\omega)}{\omega^2}\cos(\omega t)\,, \tag{B3}$$

we have, from Eqs. (B1) and (B3),

$$F(t)=-\frac{d}{dt}a(t)\,. \tag{B4}$$

Equations (B2) and (B3) lead to

$$a(t)=\frac{N}{2\omega_D^2}\int_{-\infty}^\infty d\omega\,\frac{1}{1+(\omega/\omega_D)^{2n}}e^{i\omega t}\,, \tag{B5}$$

or, with $y=\omega/\omega_D$ and $x=\omega_D t$,

$$a(t)=\frac{N}{2\omega_D}\int_{-\infty}^\infty dy\,\frac{1}{1+y^{2n}}e^{iyx} =\frac{N}{2\omega_D}\int_{-\infty}^\infty dy\,\frac{e^{iyx}}{\prod_{m=0}^{2n-1}\{y-\exp[\pi i(2m+1)/2n]\}}\,. \tag{B6}$$

The integral in Eq. (B6) can be evaluated by complex integration closing a contour in the upper half plane. The result is

$$a(t)=\frac{\pi N}{\omega_D 2^{2(n-1)}\prod_{l=1}^{n-1}\sin^2\frac{\pi l}{2n}}\begin{cases}\sum_{m=0}^{(n/2)-1}e^{-b_m x}[a_m\sin(a_m x)+b_m\cos(a_m x)]\\ \sum_{m=0}^{(n-3)/2}e^{-b_m x}[a_m\sin(a_m x)+b_m\cos(a_m x)]+\frac{1}{2}e^{-x}\end{cases}\,, \tag{B7}$$

where

$$a_m=\cos\frac{2m+1}{2n}\pi\,, \tag{B8}$$

$$b_m=\sin\frac{2m+1}{2n}\pi\,. \tag{B9}$$

From Eq. (B3), we see that $(d/dt)a(t)_{t=0}=0$ while $[-d^2a(t)/dt^2]_{t=0}=1$. These results provide us with both a consistency check and a way to fix the value of N. We obtain

$$N=2^{2(n-1)}2\sin\left(\frac{3\pi}{2n}\right)\prod_{l=1}^{n-1}\sin^2\left(\frac{\pi l}{2n}\right)\Big/\pi\omega_D\,, \tag{B10}$$

and, using Eq. (B4), we establish the result (III. 3) for $F(t)$.

APPENDIX C. AN ALGORITHM FOR THE RANDOM DISPLACEMENT FUNCTION

In this Appendix, we describe the derivation of Eqs. (III. 18)–(III. 20). These equations or the equivalent

equations (III. 21) make it possible to evaluate the random displacement functions $R_l(t)$ step by step during the integration process.

Equations (III. 17), (II. 33), and (B10) lead to

$$\langle R(t)R(0)\rangle = \phi \int_{-\infty}^{\infty} dy\, e^{iyx} \frac{1}{y^{2n}+1}, \tag{C1}$$

where

$$x = \omega_D t \tag{C2}$$

and

$$\phi = \frac{k_B T}{M} \frac{2^{2(n-1)} 2 \sin\left(\frac{3\pi}{2n}\right) \prod_{l=1}^{n-1} \sin^2\left(\frac{\pi l}{2n}\right)}{2\pi\omega_D^2}. \tag{C3}$$

We define

$$\alpha(x) = \int_{-\infty}^{\infty} dy\, e^{iyx} \frac{1}{y^{2n}+1} \tag{C4}$$

and note in passing the close relationship between α and a defined by Eq. (B5). The denominator of the integrand of Eq. (C4) can be factorized in the form

$$\begin{aligned} y^{2n}+1 &= \prod_{m=0}^{2n-1} \left[y - \exp\left(\pi i \frac{2m+1}{2n}\right)\right] \\ &= \prod_{m=0}^{n-1} \left|y - \exp\left(\pi i \frac{2m+1}{2n}\right)\right|^2, \end{aligned} \tag{C5}$$

and the integral in Eq. (C4) can be evaluated by closing a contour in the upper half plane (for $x>0$). Consider now the function

$$\begin{aligned} &\prod_{m=0}^{n-1} \left[\frac{d}{d(ix)} - \exp\{\pi i[(2m+1)/2n]\}\right] \alpha(x) \\ &= \int_{-\infty}^{\infty} dy\, e^{iyx} \frac{\prod_{m=0}^{n-1} (y - \exp\{\pi i[(2m+1)/2n]\})}{y^{2n}+1}. \end{aligned} \tag{C6}$$

The rhs of Eq. (C6) is obtained by taking the derivative of $\alpha(x)$ as defined by Eq. (C4) inside the integral. Comparing the rhs of Eq. (C6) and Eq. (C5), we see that in the integrand of Eq. (C6) all the poles on the upper half complex y plane have been eliminated and therefore the integral in Eq. (C6) vanishes.

Thus,

$$\prod_{m=0}^{n-1} \left[\frac{d}{dx} - i \exp\{\pi i[(2m+1)/2n]\}\right] \alpha(x) = 0. \tag{C7}$$

It is possible to simplify Eq. (C7) further. For this, we consider separately the cases of even and odd n. For even n, it is easy to show that

$$\begin{aligned} &\prod_{m=0}^{n-1} \left(\frac{d}{dx} - i \exp\{\pi i[(2m+1)/2n]\}\right) \\ &= \prod_{m=0}^{(n/2)-1} \left|\frac{d}{dx} - i \exp\{\pi i[(2m+1)/2n]\}\right|^2, \end{aligned} \tag{C8}$$

so that Eq. (C7) yields for this case

$$\prod_{m=0}^{(n/2)-1} \left\{\frac{d^2}{dx^2} + 2\sin\left[\frac{(2m+1)\pi}{2n}\right]\frac{d}{dx} + 1\right\} \alpha(x) = 0. \tag{C9}$$

For n odd, we obtain

$$\begin{aligned} &\prod_{m=0}^{n-1} \left(\frac{d}{dx} - i \exp\{\pi i[(2m+1)/2n]\}\right) \\ &= \left(\frac{d}{dx}+1\right) \prod_{m=0}^{(n-3)/2} \left|\frac{d}{dx} - i \exp\{\pi i[(2m+1)/2n]\}\right|^2 \end{aligned} \tag{C10}$$

and Eq. (C7) then leads to

$$\left(\frac{d}{dx}+1\right) \prod_{m=0}^{(n-3)/2} \left\{\frac{d^2}{dx^2} + 2\sin\left[\frac{(2m+1)\pi}{2n}\right]\frac{d}{dx} + 1\right\} \alpha(x) = 0. \tag{C11}$$

Denoting $\bar{R}(x) = R(t) = R(x/\omega_D)$, we see that $\langle \bar{R}(x)\bar{R}(0)\rangle = \phi\alpha(x)$ and therefore this correlation function also satisfies the differential equations (C9) or (C11). We write generally

$$L_n \langle \bar{R}(x)\bar{R}(0)\rangle = 0, \tag{C12}$$

where L_n is the linear differential operator defined by the lhs of Eq. (C7) or by the lhs of Eq. (C9) for n even and of Eq. (C11) for n odd. We now seek a stochastic differential equation of the form

$$L_n \bar{R}(x) = \rho(x), \tag{C13}$$

where $\rho(x)$ is a white Gaussian noise

$$\langle \rho(x)\rangle = 0, \tag{C14}$$

$$\langle \rho(x)\rho(x')\rangle = \bar{C}\delta(x-x'), \tag{C15}$$

so that the stochastic function $\bar{R}(x)$ which is the solution of Eq. (C13) will have the property

$$\langle \bar{R}(x)\bar{R}(x')\rangle = \phi\alpha(x-x'). \tag{C16}$$

Note that Eq. (C13) together with the fact that $\langle \rho(x)\bar{R}(0)\rangle = 0$ for $x>0$ imply that Eq. (C12) holds. In other words, Eq. (C13) is consistent with Eq. (C12) and the only remaining task is to find the correct C in Eq. (C15) which yields in Eq. (C16) the coefficient ϕ given by Eq. (C3). To this end, we start with Eq. (C13) with L_n taken in the form implied by Eq. (C7):

$$\prod_{m=0}^{n-1} \left(\frac{d}{dx} - i \exp\{\pi i[(2m+1)/n]\}\right) \bar{R}(x) = \rho(x). \tag{C17}$$

We multiply this equation by its complex conjugate written with x' as variable and then average over the distribution which determines f. We obtain

$$\prod_{k=0}^{n-1} \prod_{l=0}^{n-1} \left[\frac{d}{d(ix)} - \exp\{\pi i[(2k+1)/2n]\}\right] \left[\frac{d}{d(-ix')} - \exp\{-\pi i[(2l+1)/2n]\}\right] \langle \bar{R}(x)\bar{R}(x')\rangle = \bar{C}\delta(x-x'). \tag{C18}$$

Utilizing Eqs. (C16), (C4), and (C5), the lhs of Eq. (C18) takes the form

$$\phi \prod_{k=0}^{n-1} \left[\frac{d}{d(ix)} - \exp\{\pi i[(2k+1)/2n]\}\right] \left[\frac{d}{d(ix)} - \exp\{-\pi i[(2k+1)/2n]\}\right] \int_{-\infty}^{\infty} dy$$

$$\times \frac{\exp[iy(x-x')]}{\prod_{k=0}^{n-1}(y-\exp\{\pi i[(2k+1)/2n]\})(y-\exp\{-\pi i[(2k+1)/2n]\})} = \phi \int_{-\infty}^{\infty} dy \exp[iy(x-x')] = 2\pi\phi\delta(x-x'). \quad \text{(C19)}$$

Equations (C18) and (C19) finally yield

$$\bar{C} = 2\pi\phi. \quad \text{(C20)}$$

Equations (C13), (C14), and (C20) are equivalent to Eqs. (III. 18)–(III. 20) that we had set to prove. Note that C of Eq. (III. 20) is equal to $\bar{C}/\omega_D$, the ω_D factor resulting from the $x-t$ transformation.

[1]M. Shugard, J. C. Tully, and A. Nitzan, J. Chem. Phys. **66**, 2534 (1977).

[2]M. Shugard, J. C. Tully, and A. Nitzan, J. Chem. Phys. **69**, 336 (1978), paper I of this series.

[3]S. A. Adelman and J. D. Doll, J. Chem. Phys. **64**, 2375 (1976), and references therein.

[4](a) E. O. Siré and G. H. Kohlmaier, Ber. Bunsenges. Phys. Chem. **80**, 504 (1976); (b) G. H. Kohlmaier, E. Nowak, and E. O. Siré, Ber. Bunsenges. Phys. Chem. **80**, 515 (1976).

[5]S. A. Adelman and B. J. Garrison, J. Chem. Phys. **65**, 3751 (1976).

[6]J. D. Doll and D. R. Dion, J. Chem. Phys. **65**, 3762 (1976).

[7]M. C. Wang and G. E. Uhlenbeck, Rev. Mod. Phys. **17**, 323 (1945).

[8]For very slow rates, we sometimes used the total energy of the four atom system as a measure of the internal energy of the impurity.

[9]A. Nitzan, S. Mukamel, and J. Jortner, J. Chem. Phys. **60**, 3929 (1974); **63**, 200 (1975).

[10]M. L. Goldberger and K. M. Watson, *Collison Theory* (Wiley, New York, 1964), p. 450.